Available online at www.sciencedirect.com
ScienceDirect
Catalysis Today 119 (2007) 88–93
CATALYSIS TODAY
www.elsevier.com/locate/cattod

Detailed surface reaction mechanism for reduction of NO by CO

Dinesh Mantri, Preeti Aghalayam *

Department of Chemical Engineering, Indian Institute of Technology Bombay, Mumbai 400 076, India

Available online 11 September 2006

Abstract

In order to meet the stringent regulatory norms of NO_x and CO emitted by automobiles, reduction of these pollutants has become an intense field of research. Various catalysts like Pt, Rh, Ir, Cu, and Fe have been found to possess high activity for the reduction of NO. However, the available detailed surface reaction mechanisms are not satisfactory in clarifying all the aspects of the simultaneous reduction of NO and oxidation of CO. Here we have developed a quantitative surface reaction mechanism based on elementary steps, in order to comprehend the phenomena of catalytic reduction of NO by CO. Eleven elementary steps are proposed for the NO–CO and NO–CO–O_2 systems on Pt group catalysts. The elementary reaction mechanism is coupled with the continuously stirred tank reactor/packed bed reactor models and the simulation results are validated against literature experiments for the NO–CO reaction on Pt, and the NO–CO–O_2 reaction on Ir catalyst. Despite the simplicity, the CSTR model is able to capture the observed phenomena well on Pt and Ir catalysts. The effect of O_2 on the activity of CO for NO reduction is also analysed in detail through the simulations.

Keywords: NO reduction; Pt; Ir; Surface reaction mechanism

1. Introduction

Emissions of nitrogen oxides (NO_x) are of great concern because of their impacts on the environment, including acid rain and photochemical smog formation. Selective catalytic reduction using hydrocarbons (HC-SCR) is found to be effective for NO_x control [1–3]. The reactions between CO and NO are important in HC-SCR and CO is found to be a good reducing agent for NO_x [4–7]. The use of CO as a reducing agent has advantages for practical application because of its presence in significant amounts in automobile exhausts. CO is a poisonous gas that displaces O_2 from the blood and can exacerbate heart problems and there are strict government regulations for CO emissions. Considering all these facts, we focus our attention here on the NO–CO reaction, wherein CO is oxidized to CO_2 and NO is reduced to N_2, thus leading to the control of two of the important automotive pollutants. Use of Pt group catalysts is promising for NO_x reduction because of high hydrothermal stability, low light off temperatures and high durability in the presence of SO_2 [8,9]. Several surface reaction mechanisms (for Pt and Rh catalysts) are proposed in the literature for the reduction of NO by CO [10–13]. However, a reliable, quantitative reaction mechanism capable of capturing experimentally observed features is not available. Elementary reaction mechanisms are proposed here for the NO–CO and the NO–CO–O_2 reactions on Pt group catalysts. The reaction mechanisms are coupled with the continuously stirred tank reactor (CSTR) or the packed bed reactor (PBR) models, and the simulation results are validated using literature experimental results on Pt and Ir catalysts.

2. Elementary reaction mechanism and reactor model

There is some controversy in the literature regarding the surface reaction mechanism for the catalytic reduction of NO. Silva and Schmal [14] show that the –NCO species is an important intermediate in the NO reduction by CO while Granger et al. [6] suggest that the formation of N_2 directly from NO dissociation might be the important step for NO reduction. The literature experimental results show that N_2O is formed as an undesired product during the NO–CO reaction on Pt group catalysts [4]. Some articles indicate that N_2O is an intermediate in the formation of N_2 [5,6]. However, the formation of N_2O is not considered in many of the quantitative detailed surface reaction mechanisms proposed in literature (Oh et al. [15] on Rh (1 1 1) and Rh/Al_2O_3 catalysts, Makeeva and Kevrekidis

* Corresponding author.
E-mail address: preeti@iitb.ac.in (P. Aghalayam).

0920-5861/$ – see front matter © 2006 Elsevier B.V. All rights reserved.
doi:10.1016/j.cattod.2006.08.002

Nomenclature

av	surface area/volume of catalyst (m^2/m^3)
A_c	cross-sectional area of reactor bed (m^2)
C_i	outlet concentration of gas species i (mol/m^3)
C_i^0	inlet concentration of gas species i (mol/m^3)
R_j	rate of surface reaction j ($mol/m^2/s$)
V	volume of the reactor (m^3)
V_0	volumetric flow rate (m^3/s)
z	reactor bed length (m)
Greek letters	
θ_k	fractional coverage of surface species k
ν_{ij}	stoichiometric coefficient of species i in surface reaction j
ν_{kj}	stoichiometric coefficient of species k in surface reaction j

[16] on Pt (1 0 0), Sarkar and Khanra [17] on Pt-Rh and Pd-Rh, and so on). Considering all of the facts in literature, we propose here a surface reaction mechanism based on NO dissociation, for Pt group catalysts. The formation of N_2 directly from the combination of NO^* and N^* is proposed in a few articles [15,18–20], i.e., the reaction $NO^* + N^* \rightarrow N_2^* + O^* + {}^*$. However, this reaction is not considered in our reaction mechanism, based on the experimental observations of Belton et al. [21].

The elementary reaction steps considered here are listed in Table 1. The reaction steps are: molecular adsorption of NO, dissociation of NO^* (* refers to adsorbed species) to produce N^* and O^*, the combination of N^* with NO^* to yield N_2O and the combination of two N^* to form N_2. The O^* formed from the dissociation of NO^* combines with CO^* to give CO_2. The relevant adsorption (dissociative) and desorption steps for O_2 are also included, when O_2 is present in the feed. The activation energy for each elementary reaction on Pt (1 1 1) and Ir (1 1 1) is calculated using the unity bond index-quadratic exponential potential (UBI-QEP) method [22]. The pre-exponential factors are maintained at the order of magnitude estimates according to transition state theory, as in earlier literature [23]. The sticking coefficients for NO adsorption and O_2 adsorption over Ir catalyst are not known precisely. But a value between 0.5 and 0.7 is recommended for NO adsorption [24,25] and 0.03 for O_2 adsorption [23], over Rh and Pt catalysts. Considering this, the sticking coefficients for NO adsorption and O_2 adsorption are assumed to be 0.6 and 0.03, respectively, on both catalysts. The values of 0.92 on Ir [26] and 0.89 on Pt [23] are considered for the CO adsorption sticking coefficient. The activation energies and pre-exponential factors/sticking coefficients are also shown in Table 1, alongside the elementary reactions. Except in case of the CO adsorption step (where the sticking coefficients are slightly different for Pt and Ir), the only difference between Pt and Ir comes from the value of the activation energies, in our work.

Table 1
Proposed elementary reaction mechanism with detailed kinetic data on Pt (1 1 1) and Ir (1 1 1)

No.	Elementary reactions	Pre-exponential factor (s^{-1})/sticking coefficient	Activation energy (kcal/mol)	
			Pt (1 1 1)	Ir (1 1 1)
1	$NO + {}^* \rightarrow NO^*$	0.6	0	0
2	$NO^* \rightarrow NO^*$	1×10^{13}	26	30.7
3	$NO^* + {}^* \rightarrow N^* + O^*$	1×10^{11}	13	7.7
4	$N^* + N^* \rightarrow N_2 + 2^*$	1×10^{11}	27	39.3
5	$NO^* + N^* \rightarrow N_2O^* +$	1×10^{11}	21	28.71
6	$N_2O^* \rightarrow N_2O + {}^*$	1×10^{13}	13	14
7	$CO + {}^* \rightarrow CO^*$	0.89/0.92[a]	0	0
8	$CO^* \rightarrow CO + {}^*$	1×10^{13}	32	34
9	$CO^* + O^* \rightarrow CO_2 + 2^*$	1×10^{11}	23.7	24.9
10	$O_2 + 2^* \rightarrow 2O^*$	0.03	–	0
11	$2O^* \rightarrow O_2 + 2^*$	1×10^{11}	–	67

[a] The first and second value indicate sticking coefficient on Pt (1 1 1) and Ir (1 1 1), respectively.

The surface intermediates (adsorbed species) are assumed to be in steady state, which implies that their rate of formation is equal to their rate of disappearance. The conservation of surface sites demands that the summation of all the fractional surface coverages be one. Thus we have a simple model for the surface species consisting of a set of non-linear algebraic equations. The mass balances for the gas phase species are written using two simple reactor-scale models, namely the one-dimensional packed bed reactor (PBR) and the zero-dimensional continuously stirred tank reactor (CSTR) models as Eqs. (3a) and (3b), respectively. In both cases, the reactor is assumed to be isothermal and the dependence of reactor outlet concentrations on temperature is obtained by the simultaneous solution of these equations:

- Mass balance for surface intermediates:

$$0 = \sum_{j=1}^{nrxns} \nu_{kj} R_j \quad k = NO^*, N^*, O^*, CO^*, N_2O^* \tag{1}$$

- Site conservation:

$$1 = \sum_{k=1}^{6} \theta_k \quad k = NO^*, N^*, O^*, CO^*, N_2O^*, {}^* \tag{2}$$

- Mass balance for gas species

$$\frac{dC_i}{dz} = \text{av}\left(\frac{A_c}{V_0}\right)\left(\sum_{j=1}^{nrxns} \nu_{ij} R_j\right)$$

$$(\text{PBR model})\ (i = NO, CO, O_2, N_2O, N_2, CO_2) \tag{3a}$$

$$C_i - C_i^0 = \text{av}\left(\frac{V}{V_0}\right)\left(\sum_{j=1}^{nrxns} \nu_{ij} R_j\right)$$

$$(\text{CSTR model})\ (i = NO, CO, O_2, N_2O, N_2, CO_2). \tag{3b}$$

3. PBR/CSTR model

Although the PBR is the traditionally used model for such catalytic systems, we worked here with the CSTR model as well because the L/D ratio ($L = 14$, $D = 4$ mm [4]); ($L = 3$,

$D = 7.6$ mm [5]) of the experimental reactor beds is small. Therefore the assumptions of radial concentration uniformity and variation of concentration only in the axial direction, which are inherent in the PBR model, may be questionable. The CSTR is of course a much simpler model that ignores the spatial variation in concentration entirely, but may nevertheless be reasonable for such small catalyst beds with low values of L/D. Finally, a two-dimensional reactor model (including both axial and radial variations in concentrations and temperature) may be suggested by our results but is not attempted here as our focus is on the reaction mechanism, while keeping the reactor geometry simple.

For the packed bed reactor (PBR), the equations for the mass balance of gas phase species (Eq. (3a)) are ordinary differential equations (ODEs). These equations are coupled with six algebraic equations for the surface species (from Eqs. (1) and (2)). The system of equations is solved using MATLAB in order to obtain the outlet concentrations of various species as a function of reactor temperature, on a Pt (1 1 1) catalyst. Simulation results are compared with the experiments carried out by Chambers et al. [4] for the NO–CO reaction on a Pt/SiO_2 catalyst which is briefly described below.

Chambers et al. [4] carried out experiments on a Pt based catalyst for NO_x reduction using carbon monoxide as the reducing agent. The feed used in the experiments contained 3000 ppm NO and 3400 ppm CO. The catalytic surface area of Pt/SiO_2 is 47×10^4 m^2/m^3 and surface site density is assumed to be 1.25×10^{19} m^{-2}. It was found that at lower temperatures (<250 °C), there is no reduction of NO. NO conversion starts at 250 °C and reaches 100% at 400 °C. At lower temperatures, selectivity to N_2O was found to be higher than to N_2 and a peak was observed at 330 °C for N_2O concentration. At temperatures >330 °C, N_2 selectivity was found to increase sharply with an increase in reactor temperature. The concentration of CO was found to decrease with an increase in temperature and remain constant at high temperatures.

The concentration profiles with respect to reactor temperature are shown in Fig. 1(a), with the experimental results [4] in symbols and our simulations results using the PBR model, in lines. Good qualitative agreement is found between the simulations and the experiments. The behavior of NO reduction is found to be the same in experiments and simulations, but the temperature range where various phenomena occur is not identical with experimental data.

For the CSTR model, the mass balance of gas species (Eq. (3b)) yields non-linear algebraic equations. The set of non-linear algebraic equations obtained from Eqs. (1)–(3) are solved using MATLAB. These CSTR simulation results along with the experimental results [4] are shown in Fig. 1(b). Excellent match between the experiments and our simulations is observed. All the experimental features, including the temperature at which the conversion of NO begins, and the temperature at which N_2O concentration reaches a maximum, are quantitatively captured. Such a quantitative match between experimental results and simulations for this system is reported here for the first time. We believe that despite the simplicity, the CSTR model captures the reality better than the packed bed reactor model for these

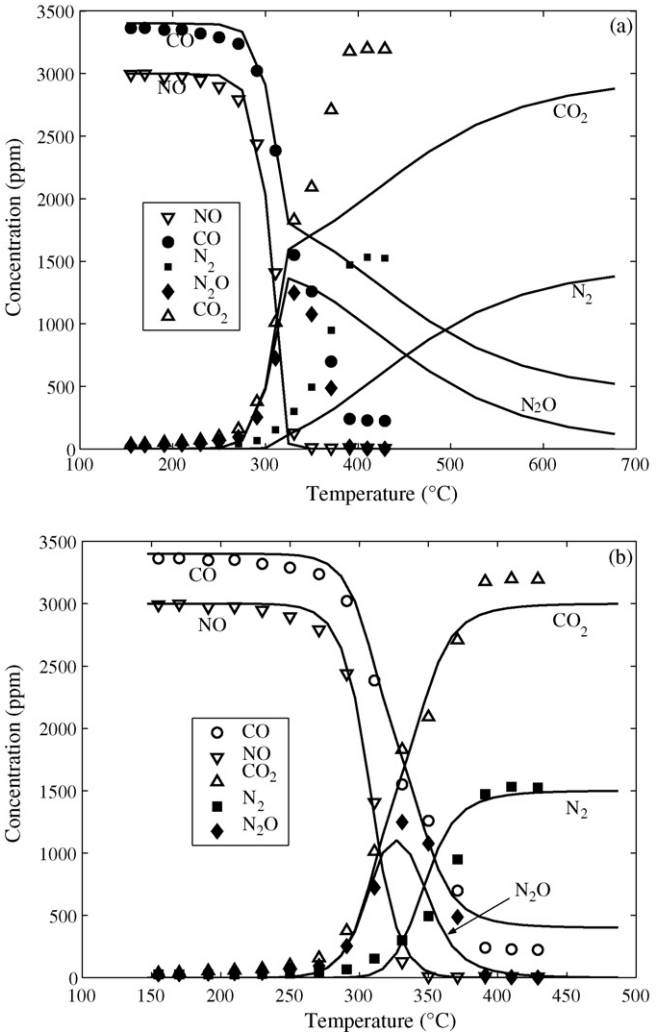

Fig. 1. Effect of temperature on the outlet concentration of gas-phase species for the NO–CO reaction on a Pt catalyst (symbols correspond to experimental data [4] on Pt/SiO_2 and lines are our simulations using (a) PBR and (b) CSTR models on Pt (1 1 1)).

experiments, because of the low L/D ratio of the experimental reactor as discussed earlier. The detailed analysis of the NO–CO system on Pt catalyst using the CSTR model is given elsewhere [27]. The available articles in the literature [5,6,12] on models for the NO–CO reaction are based on global reaction kinetics considering rate limiting step(s), and involve extensive parameter fitting. We propose here a microkinetic model involving no rate limiting step assumptions or parameter fitting, and obtain good quantitative match with literature experimental data over the full range of measured temperatures.

Thus the proposed reactor-scale model, in particular the elementary reactions mechanism on Pt, is able to capture the fundamental chemistry of the NO–CO reaction. The experimental profile of NO conversion is predicted well by both the CSTR and the PBR models. Both the models are able to capture the temperature at which the peak in N_2O concentration is observed in experiments. The CSTR model however is able to predict the concentrations at higher temperatures better than the PBR one.

4. NO–CO reactions under lean burn condition on Ir catalyst

Ir is found to be an effective catalyst with higher N_2 selectivity than Pt, Rh and Pd for the NO–CO reaction under lean burn conditions and is cheaper than Pt and Rh [28–31]. Therefore we mainly concentrate our attention on Ir rather than Pt for our analysis of NO reduction under lean burn conditions. Since the CSTR model shows good quantitative agreement with experimental results on Pt for the NO–CO reaction as shown above, simulations are performed with the same model (except that the activation energies of the reactions have different values as indicated in Table 1) on an Ir catalyst.

The simulation results obtained for the NO–CO reaction on Ir (1 1 1) for different inlet O_2 concentrations are shown in Fig. 2. In the absence of O_2, NO is almost completely converted at temperatures >400 °C with a high selectivity to N_2. The catalyst surface is mainly occupied by N^* and CO^* and the coverage of O^* is found to be negligible (Fig. 3(a)) which indicates that the catalyst is in a reduced state, leading to 100% NO conversion at high temperatures.

When O_2 is present in the feed, as the reactor temperature is increased, NO conversion first increases to reach a maximum value, after which it decreases. Thus, the effect of oxygen is that the maximum possible NO conversion is less than 100% even at high temperatures. The maximum NO conversion also decreases with increasing oxygen concentration. Above the peak temperature, NO reduction is found to be seriously depressed with an increase in the feed oxygen concentration.

Fig. 2(b) shows the effect of oxygen concentration on the conversion of CO during NO reduction. In the absence of oxygen, NO is the only oxidant for the oxidation of CO, and therefore the conversion of CO is low (<14%) even when the NO conversion is 100%, since CO is present in excess. Addition of O_2 in the feed increases the overall CO conversion considerably, with the CO being oxidized by both NO and O_2.

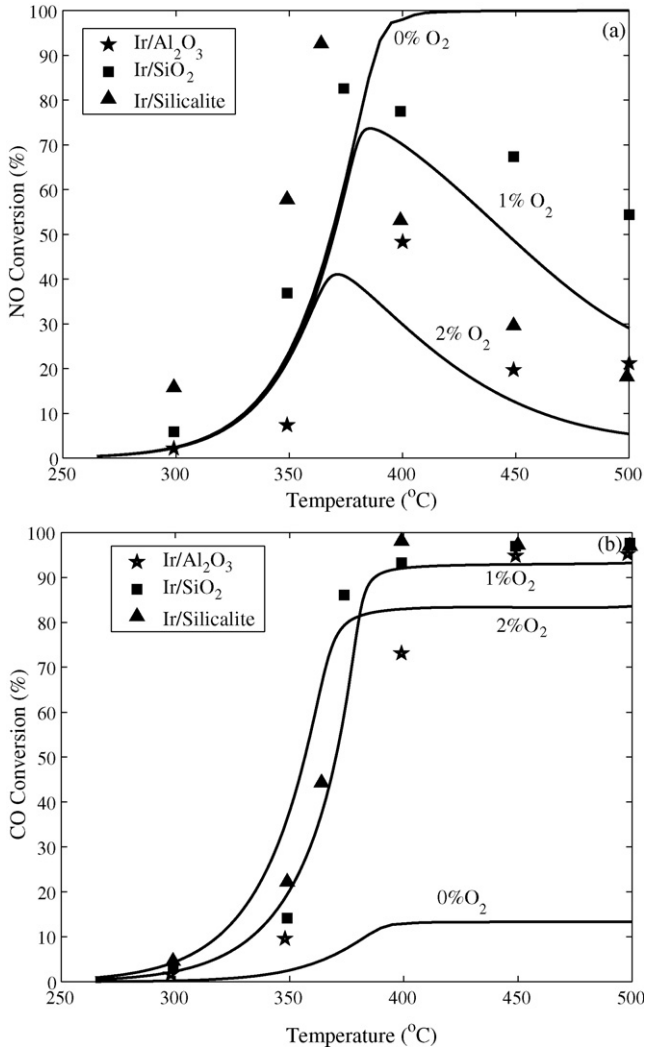

Fig. 2. Effect of reactor temperature on (a) NO conversion and (b) CO conversion for the NO–CO reaction on Ir catalyst (symbols correspond to experimental data of Ogura et al. [31] and lines are the simulations with the CSTR model on Ir(1 1 1)) (feed: 1000 ppm NO + 7500 ppm CO + O_2; experiments were done with 1% O_2).

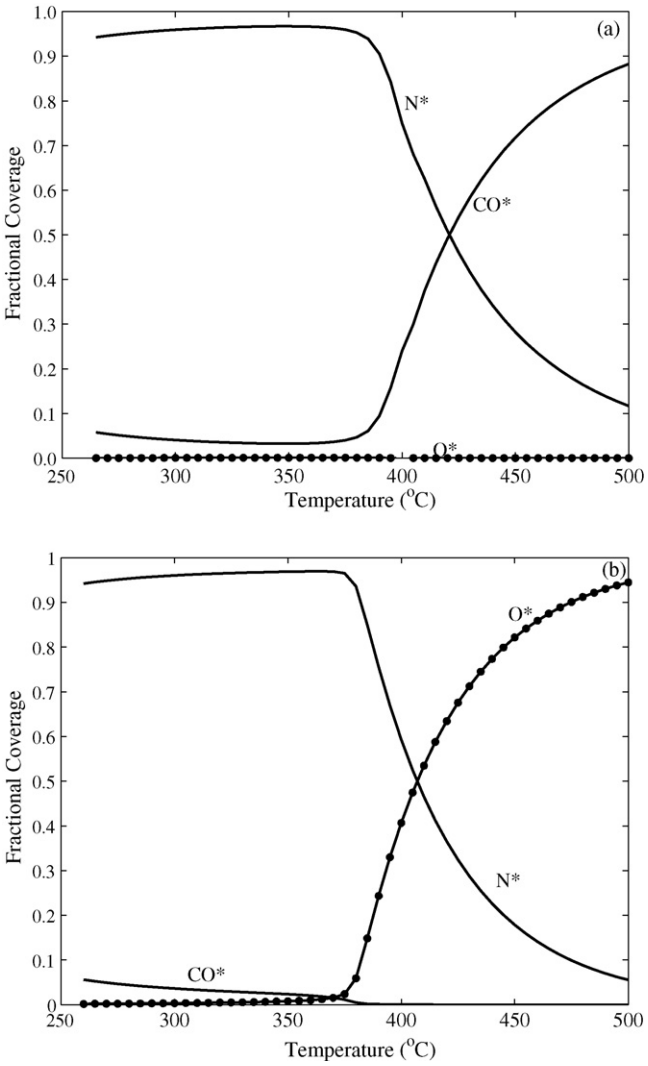

Fig. 3. Effect of reactor temperature on fractional surface coverages for the NO–CO reaction on Ir (1 1 1). (a) Feed: 1000 ppm NO + 7500 ppm CO and (b) feed: 1000 ppm NO + 7500 ppm CO + 1%O_2.

The simulation results are compared with the experimental results of Ogura et al. [31] as shown in Fig. 2. A feed condition of 1000 ppm NO + 7500 ppm CO + 1% O_2 and catalytic surface area 9.4×10^4 m^2/m^3 are used in our simulations, in line with the experiments. NO conversion begins at ~300 °C in the experiment for the three different supported (Ir/SiO_2, Ir/Al_2O_3 and Ir/silicalite) catalysts and the same is observed in our simulations for Ir (1 1 1). The NO conversion increases with temperature and reaches a maximum value, after which the NO conversion starts to decrease with a further increase in temperature. The peaks for NO conversion for Ir/SiO_2, Ir/Al_2O_3 and Ir/silicalite catalysts are observed at 400, 365 and 375 °C, respectively. In our simulations, the peak is observed at a temperature of 385 °C. Considering that the support effect is not incorporated in our simulations the results obtained are in good qualitative agreement with experiments.

It is important to note here that our simulation results match with experimental data without fitting any parameters. Furthermore, the activation energy values reported in Table 1 are calculated for the (1 1 1) surface of Pt and Ir whereas the experiments are for supported catalysts. Finally, the reactor model chosen here is a simple, isothermal CSTR. The ability to predict the experimentally observed phenomena is therefore very encouraging. We believe that this indicates that the important processes in the NO–CO reaction are quantitatively captured in the proposed surface reaction mechanism.

The typical volcano-type profile for NO conversion observed under lean-burn conditions is clearly due to the adsorption of O_2 on the catalyst. At lower temperatures when the catalyst is in a reduced state (negligible O^*), the NO conversion increases with an increase in reactor temperature. However, after a certain temperature, the O^* coverage on the surface becomes high, making the catalyst less effective for the reduction of NO. The NO conversion decreases as the O^* coverage further increases with an increase in the temperature. This shows that the presence of O_2 inhibits the catalyst activity for NO reduction at higher temperature, due to blocking of catalyst sites by O^*. In Fig. 3, the surface coverages obtained in our simulations are plotted versus the reactor temperature. Fig. 3(a) is for an NO–CO feed while Fig. 3(b) shows results for a NO–CO–O_2 feed. On comparison, it is clear that the presence of O_2 depresses the ability of the Ir catalyst to adsorb CO at higher temperatures, due to the competitive adsorption of oxygen on the surface. The surface is thus no more a 'reducing' one, which reflects in the fact that the NO conversion is low. At lower temperatures, NO can still competitively adsorb even in the presence of oxygen, and thus there is virtually no difference in either the surface coverages in Fig. 3 or in the conversions seen in Fig. 2, with and without oxygen in the feed.

5. Sensitivity analysis

To determine the important elementary reactions in the NO–CO–O_2 mechanism, sensitivity analysis is performed by changing the rate constant of each reaction by ±10%, for a feed of 1000 ppm NO, 7500 ppm CO, and 1% O_2, corresponding to the data in Fig. 2. Fig. 4 shows the NSC (normalized sensitivity coefficient) for NO conversion at three temperatures, a low temperature (350 °C), the peak temperature (385 °C, where NO conversion is a maximum, see Fig. 2) and a high temperature (450 °C). The first and second bar for each reaction indicates the NSC for −10% and +10% changes in rate constant respectively. NSC is defined as

$$\mathrm{NSC} = \frac{X_{\mathrm{NO}} - X^0_{\mathrm{NO}}}{X^0_{\mathrm{NO}}} \times 100$$

where X_{NO} indicates NO conversion for ±10% change in rate constant, X^0_{NO} indicates NO conversion for the rate constant value as noted in Table 1.

Small values of NSC indicate that the relevant reaction has almost no influence on the NO conversion. The rate constants for the reactions involving formation of N_2 and the combination of N^* and NO^* are important at low temperatures, where the

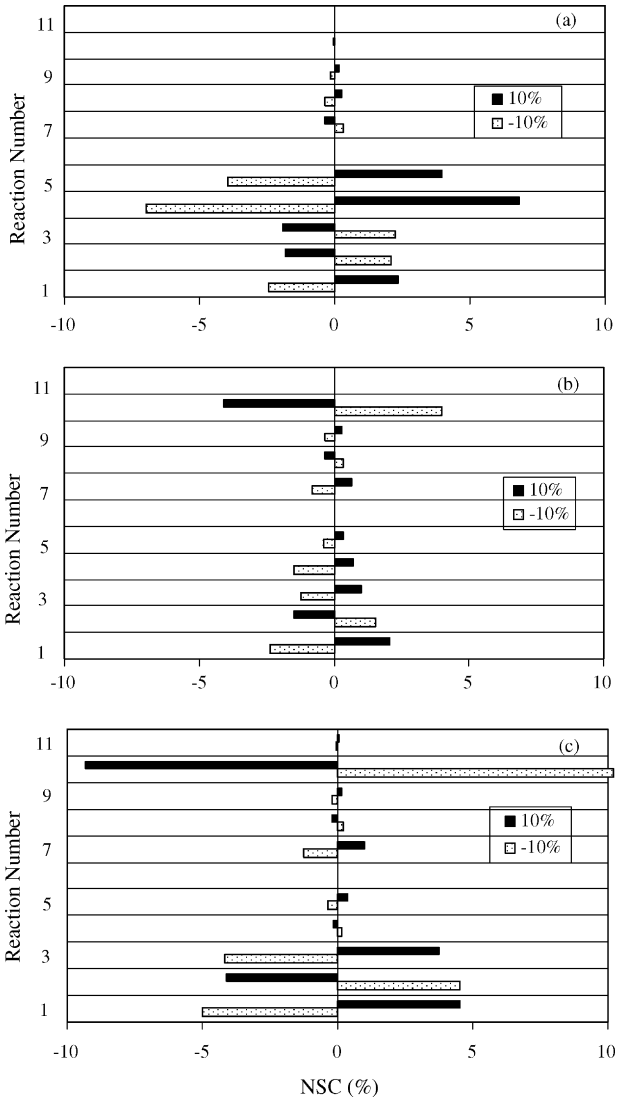

Fig. 4. Normalized sensitivity coefficient (NSC) for each elementary reaction on Ir catalyst at (a) 350 °C, (b) 385 °C and, (c) 450 °C. Conditions: 1000 ppm NO + 7500 ppm CO + 1% O_2. The bar for each reaction indicates the NSC for −10% and +10% changes in rate constant.

conversion of reactants is also low. As the temperature is increased, the O_2 adsorption reaction gains importance. The NO conversion is insensitive to O_2 adsorption at low temperatures. At the peak temperature, and beyond, the O_2 adsorption reaction becomes important in determining NO conversion. Thus for a 10% decrease in the rate constant of O_2 adsorption, a 4% increase in NO conversion is observed at 385 °C, and a 10% increase in NO conversion at 450 °C. This result is also consistent with the surface coverage data indicated in Fig. 3, which shows that the coverage of O^* increases as the temperature increases.

6. Conclusions

Detailed elementary reaction mechanisms have been developed for the NO–CO reaction on Pt and Ir catalysts, incorporating the effect of oxygen in the feed. The reaction mechanism is relevant for the catalytic reduction of NO by CO in lean-burn automotive engine applications. The simple, isothermal CSTR model incorporating the proposed detailed reaction mechanism is able to capture the experimental results better than the PBR model. The agreement between the simulations and experiments for the NO–CO and NO–CO–O_2 reactions on Pt and Ir catalysts validates the proposed surface reaction mechanism. In the absence of O_2, the catalyst is in a reduced state and complete conversion of NO is possible on both Pt and Ir catalysts, at higher temperatures. The presence of O_2 adversely affects NO reduction. The NO conversion shows a non-monotonic variation with temperature, with the decrease in conversion at higher temperatures attributable to the blocking of the catalyst sites by adsorbed oxygen. Sensitivity analysis indicates that the adsorption of O_2 is the most important reaction in the mechanism, for determining NO conversion at higher temperatures on Ir catalyst.

Acknowledgement

We are grateful to the Department of Science and Technology (DST), Govt. of India, for financial support through SERC (#03DS014).

References

[1] A. Fritz, V. Pitchon, Appl. Catal. B 13 (1997) 1.
[2] M.D. Amiridis, T. Zhang, R.J. Farrauto, Appl. Catal. B 10 (1996) 203.
[3] R. Burch, J.P. Breen, F.C. Meunier, Appl. Catal. B 39 (2002) 283.
[4] D.C. Chambers, E. Angove, W.C. Noel, J. Catal. 204 (2001) 11.
[5] P. Granger, P. Malfoy, P. Esteves, L. Leclercq, G. Leclercq, J. Catal. 187 (1999) 321.
[6] P. Granger, L. Delannoy, J.J. Lecomte, C. Dathy, H. Praliaud, L. Leclercq, G. Leclercq, J. Catal. 207 (2002) 202.
[7] P. Bera, K.C. Patil, V. Jayaram, M.S. Hegde, G.N. Subhanna, J. Mater. Chem. 9 (1999) 1801.
[8] P. Ciambelli, P. Corbo, F. Migliardini, Catal. Today 59 (2000) 279.
[9] G. Zang, T. Yamaguchi, H. Kawakami, T. Suzuki, Appl. Catal. B 1 (1992) L15.
[10] T. Fink, K. Krischer, R. Imbihl, J. Vac. Sci. Technol. 10 (4) (1992) 2440.
[11] D. Chatterjee, O. Deutschmann, J. Warnatz, Faraday Discuss. 119 (2001) 371.
[12] P. Granger, C. Dathy, J.J. Lecomte, L. Leclercq, M. Prigent, G. Mabilon, G. Leclercq, J. Catal. 173 (1998) 304.
[13] V. Bustos, C.S. Gopinath, R. Unac, F. Zaera, G. Zgrablich, J. Chem. Phys. 114 (24) (2001) 10927.
[14] M.A. Silva, M. Schmal, Catal. Today 85 (2003) 31.
[15] S.H. Oh, G.B. Fisher, J.E. Carpenter, D.W. Goodman, J. Catal. 100 (1986) 360.
[16] A.G. Makeeva, I.G. Kevrekidis, Chem. Eng. Sci. 59 (2004) 1722.
[17] A.D. Sarkar, B.C. Khanra, J. Mol. Catal. A 229 (2005) 25.
[18] W.C. Hecker, A.T. Bell, J. Catal. 84 (1983) 200.
[19] K. Cho, B.H. Shanks, J.E. Bailey, J. Catal. 115 (1989) 486.
[20] K.C. Taylor, J.C. Schlatter, J. Catal. 63 (1980) 53.
[21] N. Belton, C.L. DiMaggio, S.J. Schmieg, K.Y.S. Ng, J. Catal. 157 (1995) 559.
[22] E. Shustorovich, A.T. Bell, Surf. Sci. 289 (1993) 127.
[23] P. Aghalayam, Y.K. Park, D.G. Vlachos, AICHE.J. 46 (2000) 2017.
[24] J.H. Hoebink, R.A. Gemert, J.A. Tillaart, G.B. Marin, Chem. Eng. Sci. 55 (2000) 1573.
[25] L.H. Lin, G.A. Somorai, Surf. Sci. 107 (1981) 573.
[26] U. Burghaus, J. Ding, W.H. Weinberg, Surf. Sci. 384 (1997) L869.
[27] D. Mantri, S. Gon, S. Patel, P. Aghalayam, CHEMCON, Mumbai, India, December, 2004.
[28] L. Wang, Y. Ma, T. Cong, D. Zhang, L. Wang, Appl. Catal. B 40 (2003) 319.
[29] S.J. Tauster, L.L. Murrell, J. Catal. 41 (1976) 192.
[30] M. Shimokawabe, N. Umeda, Chem. Lett. 33 (2004) 534.
[31] M. Ogura, A. Kawamura, M. Matsukata, E. Kikuchi, Chem. Lett. (2000) 46.